Malaysian Journal of Catalysis
http://mjcat.utm.my/
MJCat
Research Article

Mesostructured TiO_2–g-C_3N_4 Hybrid Nanocomposites: A Potential Solar-Driven Solution for Textile Dye Pollution

Siti Munirah Sidik[1,2*], Mohamad Saufi Rosmi[1,2], Muhammad Shaiful Aidil Mohd Syarafuddin[1], Nurul Adilah Mohd Noor[1], Nur Farhana Jaafar[3], NurFatehah Wahyuny Che Jusoh[4], Wan Haslinda Wan Ahmad[1,2]

[1]*Department of Chemistry, Faculty of Science and Mathematics, Universiti Pendidikan Sultan Idris, 35900 Tanjong Malim, Perak, Malaysia*
[2]*Nanotechnology Research Center, Faculty of Science and Mathematics, Universiti Pendidikan Sultan Idris, 35900 Tanjong Malim, Perak, Malaysia*
[3]*School of Chemical Sciences, Universiti Sains Malaysia, 11800 Gelugor, Penang, Malaysia*
[4]*Malaysia Japan International Institute of Technology, Universiti Teknologi Malaysia, 54100 Kuala Lumpur, Malaysia*

**Corresponding Author: smunirah@fsmt.upsi.edu.my*

Article history:
Received 24 December 2025
Accepted 30 December 2025

ABSTRACT

The development of efficient solar-driven photocatalysts is crucial for sustainable treatment of dye-contaminated textile wastewater. In this study, a mesostructured titania/graphitic carbon nitride hybrid nanocomposite (MTNCN) was successfully synthesized via an impregnation method and evaluated for the photodegradation of methylene blue (MB) under UV and solar irradiation. The structural and physicochemical properties of the synthesized materials were systematically characterized using X-ray diffraction (XRD), field emission scanning electron microscopy with energy-dispersive X-ray analysis (FESEM–EDX), N_2 adsorption–desorption (BET) analysis, and UV–Vis diffuse reflectance spectroscopy (UV-Vis DRS). The XRD and FESEM–EDX results confirmed the successful incorporation and uniform distribution of CN into MTN, while preserving and enhancing the structural framework of MTN. The formation of an effective heterojunction in MTN–CN was found to enhance the textural and optical properties, significantly increasing the surface area and pore volume while reducing the particle size and band gap energy of the pristine MTN. In the photocatalytic activities, MTNCN demonstrated superior performance, achieving 78.2 % MB degradation within 30 min and 97.3 % after 180 min under solar irradiation, outperforming both pristine MTN and CN, even under UV light. This enhanced performance under solar irradiation underscores the strong potential of MTNCN as an efficient and sustainable photocatalyst for textile dye wastewater remediation.

Keywords: *mesostructured titania, graphitic carbon nitride, hybrid nanocomposite, solar-driven photocatalysis, methylene blue*

| eISSN 0128-2581 |

1. INTRODUCTION

The textile industry is one of the most water-intensive industrial sectors, generating large volumes of dye-containing wastewater during processes such as dyeing, printing, and finishing [1]. In Malaysia, where the textile sector contributes significantly to the national economy, the discharge of toxic and persistent coloured effluents poses serious threats to aquatic ecosystems, human health, and environmental sustainability [2]. Such effluents often exceed regulatory limits for key water quality parameters, including biochemical oxygen demand (BOD) and ammoniacal nitrogen [3], highlighting the urgent need for effective and sustainable wastewater treatment technologies.

Advanced oxidation processes (AOPs) have emerged as promising alternatives to conventional treatment methods due to their operational simplicity, cost-effectiveness, and ability to mineralize organic pollutants into harmless end products [4]. Among the tested catalysts, semiconductor-based photocatalysis has attracted considerable attention for wastewater remediation due to its ability to absorb light at suitable wavelengths and generate electron–hole pairs, which subsequently degrade pollutants via radical-mediated mechanisms [5]. Many semiconductors have been investigated as promising photocatalysts; however, among them, titania (TiO_2) remains the most widely used [6]. This material exhibits excellent chemical properties while being cost-effective, non-toxic, and chemically stable. Furthermore, owing to its ease of synthesis, key characteristics such as crystallinity, polymorphic composition, morphology, surface area, and particle size can be readily tailored [7].

To date, mesoporous titania nanoparticles (MTN) have shown potential as a photocatalysts owing to their high surface area, good crystallinity, and enhanced adsorption capacity. Previous study reported that MTN prepared under various aging time showed a potential as a photocatalyst in MB photodegradation [8]. However, their wide band gap (~3.2 eV) limits photoactivity to the ultraviolet (UV) region and is further hindered by rapid electron–hole recombination [9]. Graphitic carbon nitride (g-C_3N_4), a metal-free and chemically stable semiconductor with a narrower band gap (~2.7 eV), offers visible-light responsiveness and has been widely explored for photocatalytic applications [10]. Hybridizing MTN with g-C_3N_4 (CN) to form heterojunction nanocomposites is an effective strategy to enhance light absorption, improve charge separation, and boost overall photocatalytic performance.

In this study, MTNCN nanocomposites were synthesized via an impregnation method and evaluated for MB degradation under UV and simulated solar irradiation. The physicochemical properties of the photocatalysts were characterized using XRD, N_2 adsorption–desorption (BET) analysis, FESEM, and UV–Vis DRS.

2. EXPERIMENTS

2.1 Materials

Hexadecyltrimethyl-ammonium bromide (CTAB) and titanium (IV) isopropoxide (TTIP) were purchased from Sigma-Aldrich. Ammonium hydroxide (NH_4OH) and urea (CH_4N_2O) were purchased from Systerm and *n*-propanol was purchased from Bendosen. MB powder was purchased from Tunchem. All chemicals used in this research work were analytical grade and did not require any further purification.

2.2 Preparation of Catalysts

The MTN catalyst was synthesized using sol-gel method, reported earlier by [11] with some modifications. 4.68 g of CTAB surfactant was added into 720 mL distilled water, 120 mL *n*-propanol and 29 mL of 28 % ammonia solution. Then, the mixture was magnetically stirred for 30 min at 50 °C in a water bath. After 30 min, the temperature of water bath was increased to 80 °C before 5.7 mL of TTIP was added into the mixture. The solution was continued stirred for another 2 hours in water bath to allow the mixture dissolved completely. After 2 hours of stirring, the observed white solution was transferred into a container and placed in the refrigerator (5 °C) for 2 days. Then, the as-synthesized MTN solution was centrifuged at 4000 rpm to collect the gel product and dried overnight in oven at 100 °C. Finally, the product was calcined at 550 °C for 3 hours to remove the impurities.

The graphitic carbon nitride (CN) was usually synthesized using chemical route pioneered by [12]. In this study, 50 g of urea were mixed with 10 mL of distilled water and placed in a porcelain crucible with cover, and was subsequently calcined at 550 °C for 3 hours with heating rate of 2 °C/min in furnace under air atmosphere. After the calcination process, the furnace was allowed to cool to room temperature, resulting a pale-yellow powder.

The hybrid MTN and 1 wt. % CN was prepared by wet impregnation method and labelled as MTNCN. Firstly, 1 g of MTN was added to the mixture of 10 mL of distilled water and desired amount of urea (as the precursor of CN) before undergone the stirring process continuously for 10 min. After that, the mixture was placed in a porcelain crucible with cover, and was subsequently calcined at 550 °C for 3 hours with heating rate of 2 °C/min in furnace under air atmosphere. After the calcination process, the furnace was allowed to cool to room temperature.

2.3 Characterization of Mesoporous Titania Nanoparticles (MTN)

The prepared catalysts were then characterized by X-ray diffraction (XRD) analysis (Model: Rigaku MiniFlex) with Cu Kα radiation (λ = 1.5418 Å) at 2θ angle ranging from 20 ° to 80 °. The phases were identified with aid of the Joint Committee on Powder Diffraction Standards (JCPDS) library. The crystallite sizes of the synthesized catalyst were determined based on the major peak at $2\theta = 25.5$ ° using the Debye-Scherrer equation.

$$d = \frac{k\,\lambda}{\beta \cos\theta} \quad (1)$$

where d is the crystallite size, k is the shape factor (k = 0.94), λ is the wavelength of the X-ray radiation (Cu K_α = 0.1542 nm), β is the line width at half-maximum height and θ is the diffraction angle at the peak maximum [9]. The morphological properties and elements of the catalysts were examined by field-emission scanning electron microscopy (FESEM) with energy dispersive x-ray (EDX) analysis (Model: Hitachi, SU 8020, UHR). The N_2 adsorption-desorption analysis (Model: SA 3100 Surface Analyzer Beckman Coulter) was performed by using the Brunauer-Emmett Teller (BET) method which could estimate the surface area, pore volume and pore size of the catalysts. Before measurement, all samples were degassed at 300 °C and 0.1 Pa. The band gaps were measured using a PerkinElmer Lambda 900 UV- Vis DRS spectrophotometer at 300 to 800 nm wavelengths.

2.4 Photodegradation of Methylene Blue (MB)

The photodegradation was performed when 0.1 g of catalyst was added into 100 mL of MB solution and constantly stirred in a 250 mL glass vessel. Before illumination, the solution was magnetically stirred for 30 min in the dark to achieve adsorption-desorption equilibrium. Then, the reaction was continued for another 180 min with irradiation of 400W LED UV lamp (395 nm)

under continuous stirring. During the reaction, 2 mL of aliquots were sampled every 30 min and centrifuged using a micro centrifuge at 13000 rpm for 30 min to separate the liquid phase from solid catalyst before being analyzed by UV-Visible (UV-Vis) spectroscopy (Model: Jasco V-570) at λ_{max} = 665 nm [13]. The degradation percentage was calculated using the following equation;

$$\text{Degradation (\%)} = \left(\frac{C_o - C_t}{C_o}\right) \times 100 \quad (2)$$

where C_o is the initial concentration of MB before being exposed to irradiation and C_t is the concentration of MB at a specific time. The same procedure was repeated by changing the source of light irradiation to solar light.

3. RESULTS AND DISCUSSION

3.1 Physicochemical Properties of the Prepared MTN

Figure 1 showed the XRD pattern of CN, MTN and MTNCN. The XRD patterns of MTN and MTNCN showed a similar pattern with the presence of diffraction peaks at 2θ = 25.5, 38.2, 48.2, 54.3, 55.3, 63.1, 70.5, 70.7 and 75.7 ° are corresponding to the characteristic crystal planes of (101), (004), (200), (105), (211), (204), (116), (220) and (215) anatase phase, and matched well with JCPDS 21-1272 [14]. No diffraction peaks of the CN at 2θ = 27.3 ° corresponding to the (002) diffraction is detected on the MTNCN, probably due to the low loading and well distribution on the surface of the catalysts [13]. It also a noteworthy that the particle size of MTN was decreased after CN loadings from 12.44 nm to 11.80 nm, respectively.

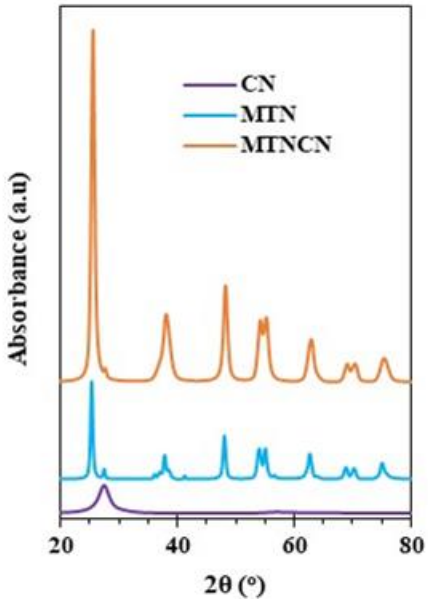

Figure 1. The XRD pattern of CN, MTN and MTNCN.

The morphology and surface characteristics of the MTNCN were demonstrated using FESEM, as illustrated in Figure 2. From the low magnification image (Figure 2 a, b), it can be seen that the MTNCN are in porous arrangement and formed abundance of deep narrow slits. A close-up image at higher magnifications (Figure 2 c, d) demonstrated that the MTNCN was made up from an aggregation of small spherical nanoparticles (less than 100 nm) forming a framework like structure with hole in the middle. This result is consistent with the morphology reported in the previous study [8], indicating that the incorporation of CN into MTN does not alter the framework structure of MTN. In fact, the increase in MTN diffraction peak intensities after CN introduction (as observed in Figure 1) suggests oriented grain growth during the incorporation of CN [15].

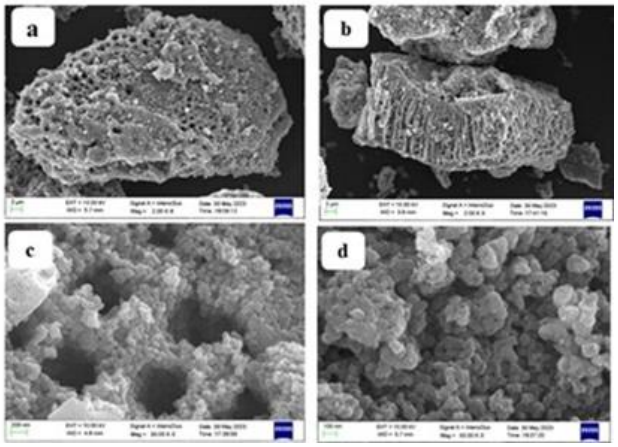

Figure 2. FESEM images of MTNCN at (a, b) 2,000, (c) 30,000 and (d) 50, 000 magnifications.

Further examination on the distribution of element on the surface of the catalyst was conducted by elemental mapping analysis, and results are shown in Figure 3.3 (a-f). Based on the analysis, there are four main elements were detected on the surface of the catalyst which is titanium (Ti), oxygen (O), nitrogen (N) and carbon (C), represented by different colored dots. The presence of uniformly distributed Ti, O, N and C elements indicated successful assembly of CN into MTN [16]. It can be observed that the signal intensity of Ti and O is much stronger than that of C and N. This phenomenon can be explained by the lower percent of CN in the MTNCN catalyst.

Table 3.1 summarizes the textural and optical properties of MTN, CN and MTNCN. According to N_2 adsorption–desorption (BET) results, the lowest surface area was found on MTN (28.66 m^2/g), followed by CN (37.49 m^2/g) and MTNCN (66.30 m^2/g). Specific surface areas and pore volume of the MTNCN is greater than those of CN and MTN, suggesting a significant quantity of CNs may promote a good dispersion of CNs in hybrids, which would benefit the expansion of certain surface areas and generation of new pores [17]. On the other hand, the pore size were decreased upon CN loading. This may be resulted from the deposition of CN particles in/on the surface of pores of the MTN, thus reducing the average pore size as compared to the MTN [18].

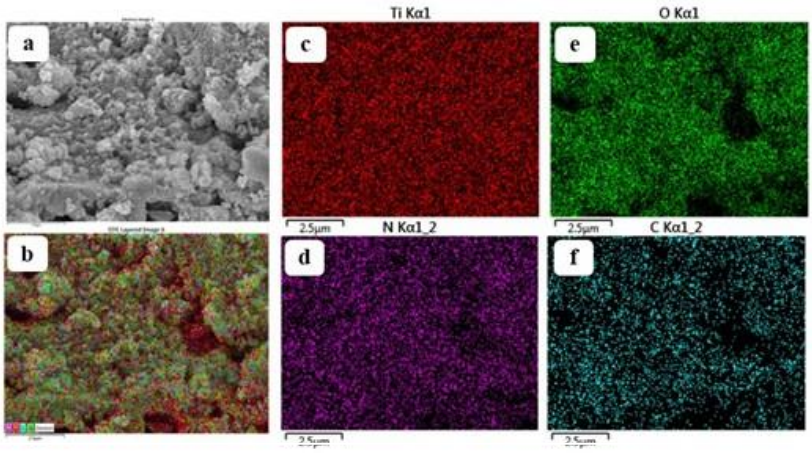

Figure 3. EDX images of (a) MTNCN, (b) multilayer (c) Ti, (d) N, (e) O, and (f) C elements.

Table 1. Textural and optical properties of MTN, CN and MTNCN 1%.

Catalyst	[a]Surface Area (m^2/g)	[a]Pore volume (cm^3/g)	[a]Pore size (cm^3/g)	[b]Particle Size (nm)	[c]Band gap (eV)
MTN	28.66	0.122	16.29	12.44	3.04
CN	37.49	0.100	13.18	n.a	2.74
MTNCN	66.30	0.182	11.17	11.80	2.94

[a] obtained from N_2 adsorption - desorption analysis using BET method.
[b] calculated using Scherer Equation using (101) peak at $2\theta = 25.5$ °
[c] determined form the plot of $[F(R)hv^{(0.5)}]$ versus photon energy (hv) using Kubelka-Munk calculation

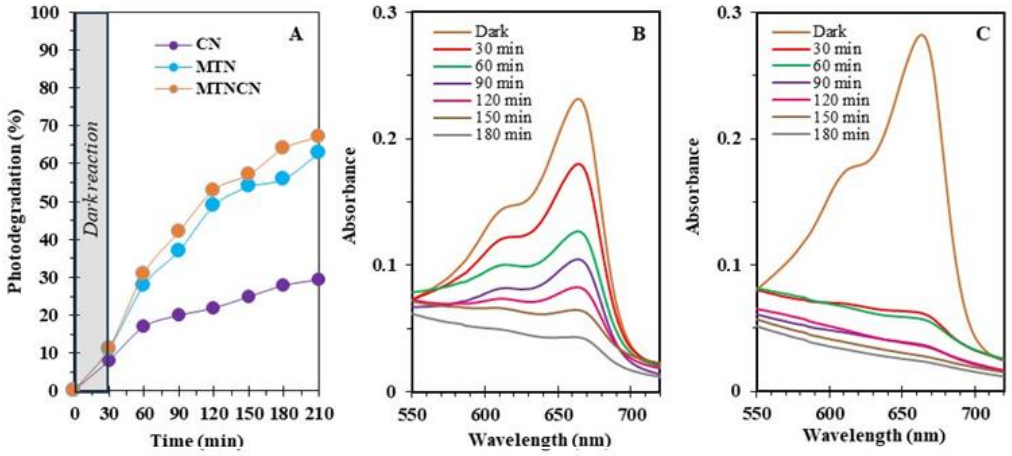

Figure 4. (A) Percentage degradation of MB using MTN, CN and MTNCN under UV light. Degradation of MTNCN under (B) UV and (C) solar irradiations.

Band gap energy determined from the extrapolation (at x-axis) of the graph edge form the plot of $[F(R)hv^{(0.5)}]$ versus photon energy (hv) for MTN, CN and MTNCN are about 3.04 eV, 2.74 eV and 2.94 eV, respectively. The result showed that the larger band gap energy of MTN (3.04 eV) was successfully lowered with the addition of CN probably due to a lower electron-hole recombination rate promoted by the heterojunction (CN-MTN) formed [19]. The decrease in band gap energy provides evidence of the system's enhanced ability to generate a greater number of active species for contaminant degradation over a broader light absorption region.

3.2 Catalytic Testing on Degradation of Methylene Blue (MB)

Figure 4 (A) shows the photocatalytic activities of the pure MTN, CN, and MTNCN in photodegradation of 100 ppm MB under UV irradiation. The first 30 minutes of reaction time, the reaction was carried out in a dark reaction

(without light irradiation) to ensure catalyst attained it adsorption-desorption equilibria. It can be seen that pure CN has the lowest activity which is only 27 % after 180 min, whereas MTN itself reaches 65.8 % of MB removal. Among all catalysts, the MTNCN sample exhibits the highest activity, showing that 67.9 % was degraded within 180 min. According to the characterization outcomes, there might have been a synergetic effect between the MTN and CN, which resulted in smaller particle size, greater surface area and a lower band gap energy. The reduction in band gap energy possibly enhances light absorption efficiency [20], thereby revealing the strong potential of MTNCN for MB photodegradation and warranting further exploration under solar irradiation.

Figure 4 shows the photodegradation of 10 ppm MB using MTNCN under (B) UV and (C) solar irradiations. MTNCN showed very high percentage of degradation under both irradiations up to 81.5 % and 97.3 %, respectively. On top of that, it was proven that better utilization of electron and hole pairs in MTNCN happen in solar irradiation. It can be clearly seen form the figures that MTNCN dramatically reduced the concentration of MB up to 78.2 % photodegradation within 30 min exposure to solar irradiation, while a much slower rate of degradation was monitored under UV light. This is because the phase junction between two different polymorphs could ease the electron transfer, thus increasing the ability to harvest the energy in solar spectrum [21]. These properties has greatly helped to shift the optical response of MTN from UV to the visible light region. Although this preliminary studies showed a significant contribution on the potential of MTNCN as a solar-driven photocatalyst in a lower concentration of MB, a detail study is worth for exploration and will be discussed in the future publication.

4. CONCLUSION

In conclusion, MTNCN was successfully synthesized via the impregnation method, and its photocatalytic performance was evaluated through the degradation of MB under different light sources. The structural and physicochemical properties of the catalysts were systematically characterized using XRD, FESEM–EDX, N_2 adsorption–desorption (BET) analysis, and UV–Vis DRS. The results confirmed the successful incorporation of CN into MTN. Moreover, MTNCN exhibited enhanced textural and optical properties, which can be attributed to the formation of a heterojunction between CN and MTN. Among all samples, MTNCN demonstrated the highest MB degradation efficiency, outperforming both MTN and CN, even under UV irradiation. Further investigation under solar light condition revealed accelerated degradation kinetics, with the most pronounced performance observed under solar irradiation, achieving 78.2 % degradation within 30 min and 97.3 % after 180 min of reaction.

ACKNOWLEDGEMENTS

We gratefully acknowledge funding support from the Kurita Water and Environment Foundation under grant number 2023-0200-101-11 and Universiti Pendidikan Sultan Idris, Perak for the resources.

REFERENCES

1. S. Varjani, P. Rakholiya, T. Shindhal, A.V. Shah, H.H. Ngo, J. Water Process Eng. 39 (2021) 101734.
2. K. Farhana, A.S.F. Mahamude, M.T. Mica, Materials Circular Economy, 4 (2022) 20.
3. A.P. Periyasamy, Cleaner Water, 4 (2025) 100092.
4. F. Tanos, E. Makhoul, A.A. Nada, M.F. Bekheet, E. Petit, A. Razzouk, G. Lesage, M. Cretin, M. Bechalany, Adv. Energy Sustainability Res., 5 (2024) 2400102.
5. N. Spigariol, L. Liccardo, E. Lushaj, E.R. Castellon, I.B. Martin, F. Polo, A. Vomiero, E. Cattaruzza, E. Moretti, Catalysis Today, 419 (2023) 114134.
6. M.R. Al-Mamun, S. Kader, M.S. Islam, M.Z.H. Khan, J. Environ. Chem. Eng. 7 (2019), 103248.
7. N. Farooq, P. Kallem, Z.U. Rehman, M.I. Khan, R.K. Gupta, T. Tahseen, Z. Mushtaq, N. Ejaz, A. Shanableh, Journal of King Saud University - Science 36 (2024) 103210.
8. S.M. Sidik, N.A.M. Noor, M.S. Rosmi, N.F. Jaafar, N. Hashim, M.N. Jajuli, Malaysian Journal of Microscopy, 20 (2024) 361.
9. M. Barik, D. Das, P.K. Satapathy, P. Mohapatra, Environ. Eng, Res. 28 (2023) 6.
10. M.A. Ahmed, S.A. Mahmoud, A.A. Mohamed, RSC Adv., 14 (2024) 25629-25662.
11. N.F. Jaafar, A.A. Jalil, S. Triwahyono, N. Shamsudin, RSC Adv., 5 (2019) 90991-91000.
12. X. Wang, K. Maeda, X. Chen, K. Takanabe, K. Domen, Y. Hou, X. Fu, M. Antonietti, J. Am. Chem. Soc. 131 (2009) 5.
13. Y.J. Acosta-Silva, R. Nava, V. Hernández-Morales, S.A. Macías-Sánchez, M.L. Gómez-Herrera, B. Pawelec, Appl. Catal. B: Eviron.110 (2011) 108-117.
14. N. Thankur, N. Thakur, J. Mater. Sci.: Mater. Electron, 35 (2024) 134.
15. S. Dey, S.C. Roy, Journal of Alloys and Compounds, 881 (2021) 160481.
16. W. Zhang, D. Xu, F. Wang, M. Chen, Nanoscale Adv., 3 (2021) 4370.
17. G. Ravi, N. Patra, S. Talu, Next Materials 9 (2025) 101128.
18. N. Fatemipayam, N. Keramati, M.M. Ghazi, Scientific Reports, 15 (2025) 8160.
19. R. Ghamarpoor, A. Fallah, N.E. Fard, S. Salehfekr, S. Hosseini, V. Moradi, Surfaces and Interfaces, 76 (2025) 107846.

20. T. Kobkeatthawin, J. Trakulmututa, T. Amornsakchai, P. Kajitvichyanukul, S.M. Smith, Catalysts, 12 (2022) 2.
21. M.G. Sahini, A. Parmain, I. Onoka, S.F. Mwanga, Journal of Alloys and Compounds, 1044 (2025) 183642.